Available online at www.sciencedirect.com
SCIENCE DIRECT®
Bioorganic & Medicinal Chemistry Letters 15 (2005) 4317–4321
Bioorganic & Medicinal Chemistry Letters

Structural elucidation of A-74528, an inhibitor for 2′,5′-phosphodiesterase isolated from *Streptomyces* sp.

Yoko Fujita, Atsushi Kasuya, Yoichi Matsushita, Miwa Suga, Masaaki Kizuka, Yasuteru Iijima and Takeshi Ogita*

Sankyo R&D Facility, Sankyo Co. Ltd., 2-58, Hiromachi 1-chome, Shinagawa-ku, Tokyo 140-8710, Japan

Received 31 May 2005; revised 14 June 2005; accepted 15 June 2005
Available online 2 August 2005

Abstract—A-74528 (**1**) is a metabolite of *Streptomyces* sp. discovered in the screening for 2′,5′-oligoadenylate phosphodiesterase inhibitors. The planar structure of **1** was mainly elucidated by NMR techniques including natural abundance INADEQUATE, and the relative configuration and the conformation were elucidated by the analyses of NOEs and assessment of dihedral angles predicted by QUANTA/CHARMm computations and coupling constants. It was proved that **1** is a highly fused polyketide with a side-chain branching site that never appeared before from the nature.

The 2-5A system is one of the major pathways involved in anti-virus and anti-tumor function that can be induced by interferons (IFNs).[1,2] 2′,5′-Oligoadenylates, unusual nucleotides (2-5A), are synthesized with several specific enzymes and bind and activate RNase L, which in turn degrades viral and cellular RNAs and thereby shuts off the protein synthesis in virus-infected cells.[3–5] The action of 2-5A is transient, however, and it is immediately deactivated by 2′,5′-specific phosphodiesterase (2′-PDE).[6–8] Therefore, it was considered that we might have an anti-viral and an anti-tumor effect if the half-life of 2-5A was prolonged by inhibiting 2′-PDE, and IFN's effect was enhanced.[9,10]

Based upon the background, we performed a screening for 2′-PDE inhibitors in microbial extracts and found a novel polycyclic polyketide, A-74528 (**1**, Fig. 1), in the culture broth of *Streptomyces* sp. SANK 61196.[11] A-74528 (**1**) inhibited the purified human 2′-PDE with an IC_{50} value of 34 μg/ml.[12] In this report, we describe the structural elucidation of **1**.

A-74528 (**1**) [UV λ_{max}(MeOH) (ε) 288 nm (19,000), 354 nm (15,400), $[\alpha]_D^{25}$ +36 (*c* 0.35 MeOH)] was isolated as a pale yellow powder and the molecular formula was determined to be $C_{30}H_{24}O_{11}$ ($[M+H]^+$, *m/z* 561.1405 Δ +0.8 mmu) by high-resolution FABMS spectral analysis.

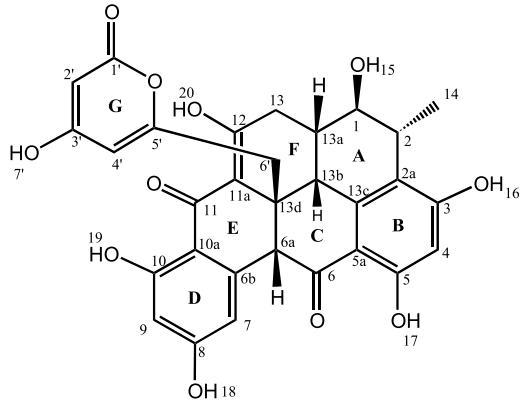

Figure 1. Structure and relative configuration of A-74528 (**1**).

The ^1H and ^{13}C NMR assignments of **1** in DMSO-d_6 at 300 K are listed in Table 1. In the ^1H NMR spectrum of **1**, the presence of six exchangeable protons (δ_H 14.80, 12.71, 11.73, 11.56, 10.90, and 10.82) suggested that **1** contained phenol and/or enol functionalities. In the ^{13}C NMR, only nine signals appeared in the aliphatic region among 30 carbons, suggesting that **1** has a highly condensed chromophore. The planar structure of **1** was elucidated mainly by the use of 2D-NMR techniques such as DQF-COSY, HSQC, and HMBC.

Keywords: Structure elucidation; Polyketide; Phosphodiesterase; A-74528; Inhibitor; Molecular-mechanics calculation; NMR.
* Corresponding author. Tel.: +81 3 3492 3131; fax: +81 3 5740 3600; e-mail: ogitak@sankyo.co.jp

0960-894X/$ - see front matter © 2005 Elsevier Ltd. All rights reserved.
doi:10.1016/j.bmcl.2005.06.047

Table 1. NMR data of A-74528 (**1**) (500 MHz, in DMSO-d_6)

No.	δ_C	δ_H
1	71.8 (d)	3.87 (1H, d, J = 3.2 Hz)
2	34.8 (d)	2.82 (1H, q, J = 7.5 Hz)
2a	118.8 (s)	
3	164.5 (s)	
OH-16		10.90 (1H, br s)
4	100.7 (d)	6.22 (1H, s)
5	163.1 (s)	
OH-17		12.71 (1H, s)
5a	108.7 (s)	
6	198.5 (s)	
6a	53.3 (d)	4.23 (1H, s)
6b	141.0 (s)	
7	113.6 (d)	6.40 (1H, d, J = 2.2 Hz)
8	164.7 (s)	
OH-18		10.82 (1H, br s)
9	101.8 (d)	6.20 (1H, d, J = 2.2 Hz)
10	163.9 (s)	
OH-19		11.73 (1H, br s)
10a	107.2 (s)	
11	189.2 (s)	
11a	106.3 (s)	
12	178.1 (s)	
OH-20		14.80 (1H, s)
13	29.0 (t)	2.33 (1H, dd, J = 19.1, 12.0 Hz)
		2.49 (1H, dd, J = 19.1, 6.1 Hz)
13a	31.5 (d)	2.94 (1H, m)
13b	32.9 (d)	3.50 (1H, d, J = 3.4 Hz)
13c	139.0 (s)	
13d	42.0 (s)*	
14	20.7 (q)	1.34 (3H, d, J = 7.5 Hz)
1′	163.5 (s)	
2′	89.0 (d)	5.18 (1H, d, J = 1.8 Hz)
3′	169.9 (s)	
OH-7′		11.56 (1H, br s)
4′	104.1 (d)	5.94 (1H, d, J = 1.8 Hz)
5′	161.7 (s)	
6′	42.0 (d)*	2.65 (1H, d, J = 14.7 Hz)
		2.98 (1H, d, J = 14.7 Hz)

* Signal overlapping.

Partial structure a. The presence of an α-pyrone moiety was readily deduced by the allyl coupling between olefinic protons at δ_H 5.18 (H-2′) and 5.94 (H-4′) and the HMBC correlations from these two protons as shown in Figure 2a. The chemical shifts C-1′, C-3′, and C-5′ (δ_C 163.5, 169.9, and 161.7, respectively) indicated that these carbons are carbonyls or oxygen-bearing olefinic carbons. Further confirmation of the partial structure was achieved by the comparison of NMR data of the 4-hydroxy-6-methyl-2 pyrone[13] in which the chemical shifts of the carbon in the partial structure were in good agreement with literature values, δ_C 164.4 (C-1), δ_C 88.5 (C-2), δ_C 170.6 (C-3), δ_C 100.4 (C-4), and δ_C 162.6 (C-5).

Partial structure b. The DQF-COSY spectrum revealed two sets of substructures, between C-2 and C-14 and between C-13 and C-13b, including oxymethine C-1 as a branched chain as shown in Figure 2b. These two substructures were connected through C-1 and C-2 based on the long-range correlations in the HMBC experiments. The partial structure was further extended based on the results of the HMBC experiments: long-range correlations of H-13b to a quaternary carbon at δ_C 42.0 (C-13d) and an olefinic quaternary carbon at δ_C 106.3 (C-11a), as well as those of methylene protons (H-13) to olefinic quaternary carbons at δ_C 178.1 (C-12) and C-11a suggested the existence of a cyclohexene ring consisting of C-13a, C-13, C-12, C-11a, C-13d, and C-13b.

Partial structure c. The presence of a resorcinol moiety was suggested based on the results of the long-range correlations of two phenolic protons at δ_H 10.82 (OH-18) and 11.73 (OH-19), and *meta*-coupled aromatic protons at δ_H 6.40 (H-7) and 6.20 (H-9) as shown in Figure 2c. C-10a was assigned to a carbon adjacent to C-10 based on the ^1H–^{13}C long-range correlations of OH-19, H-7, and H-9. Furthermore, a methine proton at δ_H 4.23 (H-6a) revealed long-range couplings to carbons at C-6b, C-10a, and C-7 suggesting that C-6b is a member of the benzene ring and C-6a is located on the benzylic position (Fig. 2c).

Partial structure d. Another resorcinol moiety was suggested by the long-range couplings shown in Figure 2d, i.e., those between the phenolic proton at OH-16 and C-3 or C-4, the aromatic proton at δ_H 6.22 (H-4) and C-2a, C-3, C-5 or C-5a, and the phenolic proton at OH-17 and C-4 or C-5a. The last member of the aromatic ring was deduced to be an aromatic quaternary carbon at δ_C 139.0 (C-13c). Although no long-range coupling was observed for the carbon, as this is the only aromatic carbon left, it was considered to occupy this position.

Connection of partial structures. The ^{13}C NMR spectrum in DMSO-d_6 revealed 29 peaks for 30 carbons indicating that one of the peaks was an overlap of two signals. Then, the ^{13}C NMR spectrum was obtained using benzene-d_6/methanol-d_4 (1:1) as a solvent. In the spectrum, 30 carbon signals were observed and an aliphatic methylene signal at δ_H 42.0, which overlapped with the C-13d

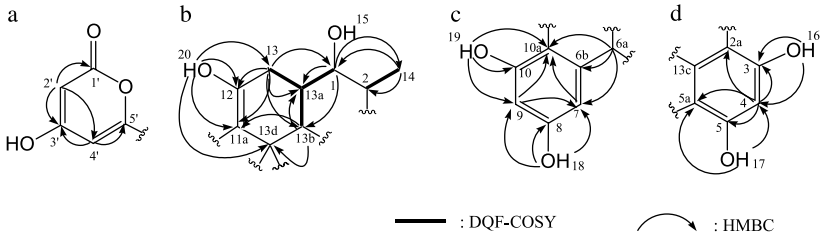

Figure 2. Partial structure of **1**.

quaternary carbon in the spectrum of DMSO-d_6, was detected. In the HMBC spectrum taken in benzene-d_6/methanol-d_4 (1:1), the long-range correlations between C-6′ and H-4′ and between C-5′ or C-13d and H-6′ were observed. These findings suggested that the partial structures a and b should be connected through the C-6′ methylene carbon as depicted in Figure 3. The long-range couplings between H-1 and C-2a, and H-2 and C-2a or C-13c as well as those between H-13b and C-2a firmly established the linkage between partial structures b and d. For the carbonyl carbon at δ_C 198.5 (C-6), which was not associated with any of the partial structures, long-range correlations with H-4 (4 bond), H-6a, and H-7 (4 bond) were observed. Taking into consideration the chemical shifts of adjacent carbons and protons, it is reasonable to conclude that the carbonyl carbon is located between partial structures c and d. The carbonyl carbon at δ_C 189.2 (C-11) turned out to be located next to C-10a, based on the HMBC correlations with H-7 and H-9 (4 bond). Although no major correlation was observed in the HMBC experiment aside from these signals, C-11 carbonyl carbon may be assigned to the position adjacent to C-11a since it represents a single carbon with no determined connectivity. The chemical shifts of these carbons were compatible with the putative structure as shown in Figure 3.

To confirm the putative structure, the 2D-INADEQUATE spectrum of **1** was taken in natural abundance using a Bruker AVANCE-500 spectrometer equipped with a cryogenic probe.[14] In the spectrum, the two crucial carbon–carbon linkages, C-6 to C-6a and C-11 to C-11a, that could not be proven directly based on the HMBC spectrum were firmly established. Furthermore, all other carbon–carbon correlations observed in the 2D-INADEQUATE spectrum were also in accord with the putative structure.

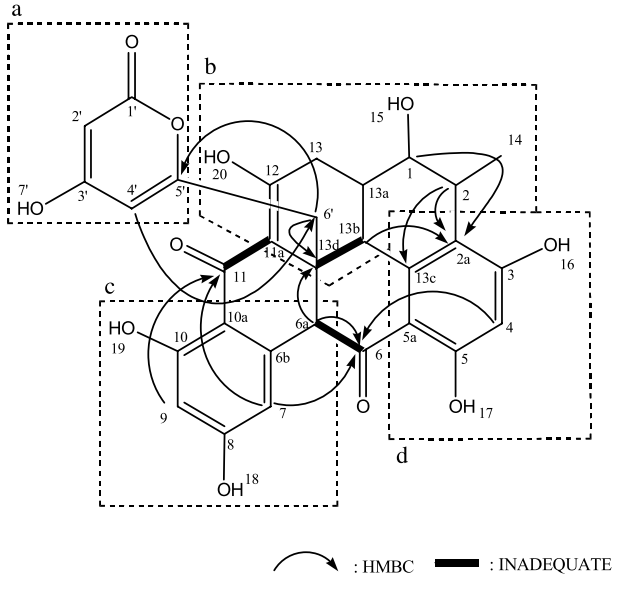

Figure 3. Connectivities of partial structures revealed by HMBC and INADEQUATE spectra in benzene-d_6/methanol-d_4 (1:1).

Based on these results, the gross structure of **1** was elucidated as illustrated in Figure 1.

Elucidation of the relative configuration of six asymmetric carbons. The relative configurations of six asymmetric carbons, C-1, C-2, C-6a, C-13a, C-13b, and C-13d, were elucidated by ROESY experiments as well as an assessment of the proton–proton dihedral angles obtained from the coupling constant data. First, the NOE correlation observed between H-13a and H-13b, which are located at the ring junctions of rings A and F, revealed that these rings were fused in a *cis* fashion (Fig. 4). Second, the α-pyrone moiety connected to the ring junction of rings C, E, and F was suggested to be in *syn*-pseudodiaxial relationship with respect to H-13a on the cyclohexene ring F, based on the NOE correlations between H-4′ and H-13a or H-13b as well as the structural restriction of rings C, E, and F. Furthermore, H-6a also turned out to be present in the *syn* configuration relative to the α-pyrone moiety on rings C and E, based on the NOE correlation between H-6a and H-13b. These results suggested that rings A and F and C and E were all fused in the *cis* fashion to each other, and, consequently, the relative configurations of C-6a, C-13a, C-13b, and C-13d were determined to be *S*′, *S*′, *S*′, and *R*′, respectively.

The stereochemistry of C-1 and C-2 was elucidated by taking two conformers of ring A into consideration as shown in Figure 5. Regarding that of C-2, a characteristic NOE signal was observed between the axial proton of H-13 (H-13$_\alpha$) and the protons of the H-14 methyl group, a substituent of C-2. This finding suggested that ring A adopted a pseudochair conformation and the methyl group should occupy the α-axial position. Therefore, the relative configuration of C-2 was assigned to be *R*′. As for the stereochemistry of C-1, two key NOE correlations, i.e., those between H-14 and H-1 and H-1 and H-13$_\beta$, were further observed. Since these signals were accounted for only when the H-1 was in the α-equatorial position as shown in Figure 5b, the relative stereochemistry of C-1 was deduced to be *R*′.

To confirm the conformation of ring A and the stereochemistry of C-1, the energy-minimized calculation was conducted by QUANTA/CHARMm computations, while considering $J_{H1,2}$ and $J_{H1,13a}$.[15,16] As shown in

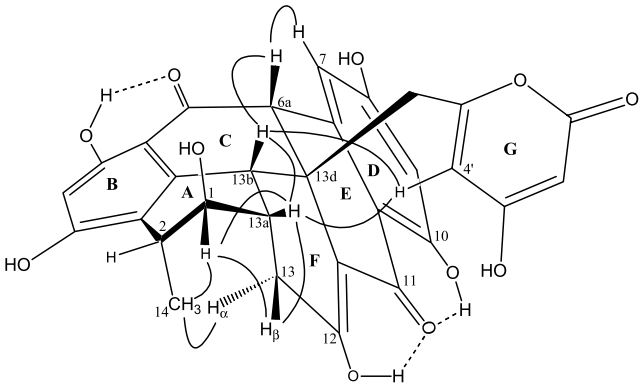

Figure 4. Stereochemical view of **1** and NOE correlations.

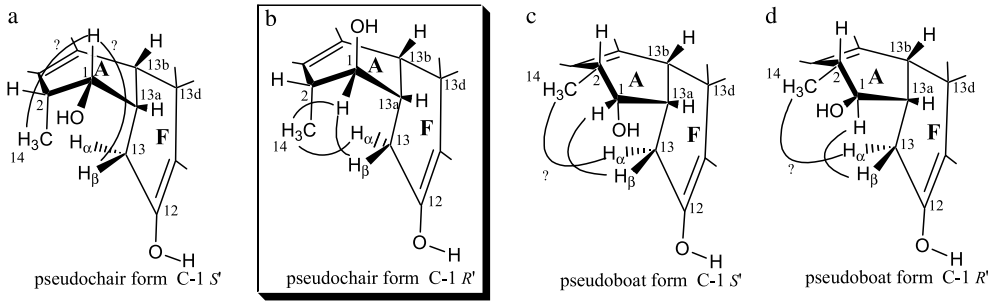

Figure 5. Possible structures of A/F ring and NOE correlations.

Table 2, the dihedral angle values of H-1–C-1–C-2–H-2 were −25.9°, −38.4°, and 155.7° in the models of 1*S*′ pseudochair (Fig. 5a), 1*S*′ pseudoboat (Fig. 5c), and 1*R*′ pseudoboat (Fig. 5d), respectively, which conflicted with the dihedral angle of 70–100°, derived from the observed *J* value (<1 Hz). On the contrary, the dihedral angle 91.6° of the 1*R*′ pseudochair model (Fig. 5b) agreed well with the observations. Furthermore, the dihedral angles H-1–C-1–C-13a–H-13a and H-13a–C-13a–C-13b–H-13b of the same model also agreed with those from the observed *J* value. These results demonstrated that the conformation of ring A was in the pseudochair form and the stereochemistry of C-1 was *R*′. In addition, as shown in Table 2, the calculated proton distance between H-13$_\alpha$ and H-14 (=4.0 Å) conflicted with the observed NOE correlation in both pseudoboat models (Figs. 5c and d). In the 1*S*′ pseudochair model, those between H-1 and H-13$_\beta$ (=3.9 Å) and between H-1 and H-14 (=3.5 Å) also conflicted with the observed NOE correlations. Only in the 1*R*′ pseudochair model, these proton distance were reasonable for the observed NOE correlation (<2.8 Å). These results also supported the conclusion that the stereochemistry of C-1 is *R*′. It should be noted that the potential energies obtained for the pseudochair models were lower than those for the pseudoboat models, suggesting that the pseudochair conformation was more stable.

Hence, the relative stereochemistry of **1** was determined to be 1*R*′, 2*R*′, 6a*S*′, 13a*S*′, 13b*S*′, and 13d*R*′, as shown in Figure 1.

The determination of the absolute configuration could not be realized since any attempt to crystallize the compound for an X-ray crystallographic study failed. Furthermore, the compound was inert and/or unstable for a chemical modification such as application of the modified Mosher's method.[17] Although we failed to determine the absolute configuration, the conformation of **1** could be predicted based on QUANTA/CHARMm computations. In that model, rings A, B, and C, and rings D, E, and F, were roughly in the same planes, which were connected at angles of about 90°. Hence, **1** was elucidated as a unique structure with an α-pyrone moiety extending on the top of a "roof" consisting of two planes.

Table 2. Dihedral angles and proton–proton distances of computationally derived models and observed coupling constant

Dihedral angles ring A						
Initial conformation	C-1	H-1–C-1–C-2–H-2	H-1–C-1–C-13a–H-13a	H-13a–C-13a–C-13b–H-13b	Potential energy (kcal/mol.)	
Pseudochair	1*S*′	−25.9	57.0	−62.0	20.999	
	1*R*′	91.6	−59.6	−63.5	17.887	
Pseudoboat	1*S*′	−38.4	18.5	−62.3	21.433	
	1*R*′	155.7	−98.5	−62.4	19.532	
Proton–proton distance (Å)						
Initial conformation	C-1	H-1–H-14	H-1–H-13$_\beta$	H-13$_\alpha$–H-14	H-6a– H-13b	H-6a–H-7
Pseudochair	1*S*′	3.46	3.86	2.11	2.64	2.36
	1*R*′	2.27	2.77	2.12	2.66	2.36
Pseudoboat	1*S*′	2.63	3.49	3.99	2.70	2.36
	1*R*′	2.57	2.53	4.02	2.71	2.36
Observed coupling constant						
	Observed coupling constant (Hz)	Dihedral angle (°)				
$J_{H1–2}$	<1	70–100				
$J_{H1–13a}$	2.0	60 or 105				
$J_{H13a–13b}$	3.6	50 or 110				

Supplementary data

2D-INADEQUATE spectrum in natural abundance and the details of QUANTA/CHARMm computations. Supplementary data associated with this article can be found in the online version at doi:10.1016/j.bmcl.2005.06.047.

References and notes

1. Player, M. R.; Torrence, P. F. *Pharmacol. Ther.* **1998**, *78*, 55.
2. Kerr, I. M.; Brown, R. E. *Proc. Natl. Acad. Sci. U.S.A.* **1978**, *75*, 256.
3. Rebouillat, D.; Hovanessian, A. G. *J. Interferon Cytokine Res.* **1999**, *19*, 295.
4. Schmidt, A.; Zilberstein, A.; Shulman, L.; Federman, P.; Berissi, H.; Revel, M. *FEBS Lett.* **1978**, *95*, 257.
5. Zhou, A.; Hassel, B. A.; Silverman, R. H. *Cell* **1993**, *72*, 753.
6. Williams, B. R. G.; Kerr, I. M.; Gilbert, C. S.; White, C. N.; Ball, L. A. *Eur. J. Biochem.* **1978**, *92*, 455.
7. Schmidt, A.; Chernajovsky, Y.; Shulman, L.; Federman, P.; Berissi, H.; Revel, M. *Proc. Natl. Acad. Sci. U.S.A.* **1979**, *76*, 4788.
8. Johnston, M. I.; Hearl, W. G. *J. Biol. Chem.* **1987**, *262*, 8377.
9. Silverman, R. H. *Biochemistry* **2003**, *42*, 1805.
10. Carpten, J.; Nupponen, N.; Isaacs, S.; Sood, R.; Robbins, C.; Xu, J.; Faruque, M.; Moses, T.; Ewing, C.; Gillanders, E.; Hu, P.; Bujnovszky, P.; Makalowska, I.; Baffoe-Bonnie, A.; Faith, D.; Smith, J.; Stephen, D.; Wiley, K.; Brownstein, M.; Gildea, D.; Kelly, B.; Jenkins, R.; Hostetter, G.; Matikainen, M.; Schleutker, J.; Klinger, K.; Connors, T.; Xiang, Y.; Wang, Z.; De Marzo, A.; Papadopoulos, N.; Kallioniemi, O. P.; Burk, R.; Meyers, D.; Gronberg, H.; Meltzer, P.; Silverman, R.; Bailey-Wilson, J.; Walsh, P.; Issacs, W.; Trent, J. *Nat. Genet* **2002**, *30*, 181.
11. The isolation and fermentation of A-74528 will be reported soon elsewhere.
12. Kubota, K.; Nakahara, K.; Ohtsuka, T.; Yoshida, S.; Kawaguchi, J.; Fujita, Y.; Ozeki, Y.; Hara, A.; Yoshimura, C.; Furukawa, H.; Haruyama, H.; Ichikawa, K.; Yamashita, M.; Matsuoka, T.; Iijima, Y. *J. Biol. Chem* **2004**, *279*, 37832.
13. Pouchet, C. J.; Behnke, J. *The Aldrich Library of ^{13}C and ^{1}H FT NMR Spectra*, 1st ed.; Aldrich Chemical Company: U.S.A., 1993; Vol. 1, 1158C.
14. See supplementary data.
15. See supplementary data.
16. QUANTA2000/CHARMm25.2, 2000, Accelrys Inc., San Diego, California.
17. Ohtani, I.; Kusumi, T.; Kashman, Y.; Kakisawa, H. *J. Am. Chem. Soc.* **1991**, *113*, 4092.